



## Comparison of two inverse analysis techniques for learning deep excavation response

Youssef M.A. Hashash<sup>a,\*</sup>, Séverine Levasseur<sup>b,1</sup>, Abdolreza Osouli<sup>a</sup>, Richard Finno<sup>c</sup>, Yann Malecot<sup>d,2</sup>

<sup>a</sup> Department of Civil and Environmental Engineering, University of Illinois at Urbana-Champaign, 205 North Mathews, Urbana, IL 61801, United States

<sup>b</sup> National Foundation of Scientific Research in Belgium, University of Liege, Department ArGEnCo Geomechanical and Geological Engineering, Chemin des chevreaux 1, 4000 Liege 1, Belgium

<sup>c</sup> Department of Civil and Environmental Engineering, Northwestern University, Evanston, IL 60208, United States

<sup>d</sup> Université Joseph Fourier – Grenoble I, Laboratoire Sols Solides Structures – Risques, BP, 53-38041 Grenoble cedex 9, France

### ARTICLE INFO

#### Article history:

Received 27 March 2009

Received in revised form 14 October 2009

Accepted 23 November 2009

Available online 29 December 2009

#### Keywords:

Excavation

Inverse analysis

Optimization

Soil behavior

Neural network material models

### ABSTRACT

Performance observation is a necessary part of the design and construction process in geotechnical engineering. For deep urban excavations, empirical and numerical methods are used to predict potential deformations and their impacts on surrounding structures. Two inverse analysis approaches are described and compared for an excavation project in downtown Chicago. The first approach is a parameter optimization approach based on genetic algorithm (GA). GA is a stochastic global search technique for optimizing an objective function with linear or non-linear constraints. The second approach, self-learning simulations (SelfSim), is an inverse analysis technique that combines finite element method, continuously evolving material models, and field measurements. The optimization based on genetic algorithm approach identifies material properties of an existing soil model, and SelfSim approach extracts the underlying soil behavior unconstrained by a specific assumption on soil constitutive behavior. The two inverse analysis approaches capture well lateral wall deflections and maximum surface settlements. The GA optimization approach tends to overpredict surface settlements at some distance from the excavation as it is constrained by a specific form of the material constitutive model (i.e. hardening soil model); while the surface settlements computed using SelfSim approach match the observed ones due to its ability to learn small strain non-linearity of soil implied in the measured settlements.

© 2009 Elsevier Ltd. All rights reserved.

### 1. Introduction

Construction of deep excavations in urban environments often raises significant concerns related to induced ground movements and potential damage to adjacent buildings. Therefore it is critically important to estimate and control the magnitude and distribution of ground movements that result from developing underground space.

In practice, observational programs are set up at construction sites to evaluate design assumptions, determine causes of failure, improve the construction procedure, determine the need for immediate repair, evaluate the stability of construction, and at times to satisfy regulatory requirements. In the course of excavation projects, civil engineers rely heavily on field data to evaluate current construction conditions and make necessary adjustments

to the construction activities as needed. Often, such evaluations are done by applying field data to numerical models, especially when the complexity of an analysis extends beyond the use of engineering judgment.

Inverse analyses have been applied to geotechnical problems for several decades [8,19,23,40]. These techniques allow engineers to evaluate numerically performance of geotechnical structures by a quantifiable observational method. Inverse analyses have been used to identify soil parameters from laboratory or in situ tests [2,41,48], performance data from excavation support systems [6,24,36], excavation of tunnels in rock [13,18,40], and embankment construction on soft soils [3,26].

The successful use of numerical simulations in geotechnical engineering is highly dependent on the constitutive model chosen to represent soil behavior. The field of constitutive relations has over the past decade been extended beyond classical elastoplastic theories to soft computing methods. Ghaboussi and his co-workers [15,17] show that artificial neural network (ANN) can represent material constitutive response including soils. ANNs fall within the broader category of soft computing methods inspired by biological computational methods [14,47]. These methods learn and evolve as information becomes available.

\* Corresponding author. Tel.: +1 217 333 6986; fax: +1 217 333 9464.

E-mail addresses: [hashash@illinois.edu](mailto:hashash@illinois.edu) (Y.M.A. Hashash), [severine.levasseur@ulg.ac.be](mailto:severine.levasseur@ulg.ac.be) (S. Levasseur), [aosouli2@illinois.edu](mailto:aosouli2@illinois.edu) (A. Osouli), [finno@northwestern.edu](mailto:finno@northwestern.edu) (R. Finno), [yann.malecot@ujf-grenoble.fr](mailto:yann.malecot@ujf-grenoble.fr) (Y. Malecot).

<sup>1</sup> Tel.: +32 (0)366 93 26.

<sup>2</sup> Tel.: +33 (0)4 76 82 70 44; fax: +33 (0)4 76 82 70 00.

In this paper the performance of two inverse analysis techniques in capturing observed performance of a deep excavation in downtown Chicago are compared. The first method is based on a genetic algorithm (GA) optimization method. Its goal is to identify soil parameters of a constitutive model from in situ measurements. The second method is based on artificial neural networks (ANN). Its goal is to extract soil behavior from experimental data without a pre-defined constitutive model. Both inverse analysis techniques and their application to a deep excavation in downtown Chicago are described in the following sections. Each method has been presented in previous studies as very efficient methods to solve excavation inverse analysis problem [23,31,32]. This paper compares the performance of both techniques in capturing soil displacements and in predicting of soil behavior (stress path) in Lurie Center excavation in Chicago, Illinois, USA.

## 2. Inverse analysis techniques

### 2.1. System identification: error minimization and genetic algorithms

The proposed identification method is used to study the soil behavior in Lurie Center deep excavation, based on the inverse analysis theory introduced by Tarantola [45]. This method establishes a suitable identification method to adapt itself to different kinds of geotechnical measurements such as pressuremeter curves or displacement of retaining walls [30].

The inverse analysis is based on a genetic algorithm optimization process (GA) used to identify soil parameters. This method is well known as a robust and efficient approach to solve complex problems [20]. Genetic algorithm can find the optimal solution of the problem even with a flat or noisy error function [30]. This optimization process also provides information on the existence of correlations between parameters. Moreover, usually in inverse analysis of geotechnical problems due to modeling errors or in situ measurement uncertainties, rather than only one exact solution, several approximate solutions exist. Levasseur et al. [31,32] have shown that a genetic algorithm in combination with a statistical analysis, such as a principal component analysis, is able to identify many of these approximate solutions of the inverse analysis problem. The main drawback of this method is the high calculation cost. For instance, in an excavation problem requiring identification of three soil model parameter, it takes about 2 days with an office computer. It is necessary to perform many finite element calculations at the beginning of the optimization process to have a good estimation of the error function in the search space. This sweep, which is essential for the genetic algorithm, makes this method computationally expensive [29]. However, as computational costs reduce, this drawback will become less an issue.

The application of this method in excavation problems is shown in Fig. 1. Trial values of the unknown soil model parameters are used as input values in a finite element code to simulate the excavation problem. PLAXIS [39] is used as the finite element engine in this study. The computed lateral wall deflections and surface settlements are compared to measured values. If the discrepancy between measured and computed results is not in an acceptable range, then the input soil model parameters are optimized using the genetic algorithm (GA). This process is repeated until a good match between computed and measured soil behavior is observed. Then the identified solution sets are interpreted through a statistical approach, principal component analysis (PCA) [27].

#### 2.1.1. Identification method

**2.1.1.1. Error function.** The discrepancy between the measured behavior and the modeled one is expressed by a scalar error function,  $F_{err}$  in the sense of the least square method as introduced by Levasseur et al. [30]:

$$F_{err} = \left( \frac{1}{N} \sum_{i=1}^N \frac{(Ue_i - Un_i)^2}{\Delta U_i^2} \right)^{1/2} \quad (1)$$

where  $N$  is the number of measurement points,  $Ue_i$  the  $i$ th measured value,  $Un_i$  the corresponding value of the numerical calculation and  $1/\Delta U_i$  the weight of the discrepancy between  $Ue_i$  and  $Un_i$ .  $1/\Delta U_i$  is equal to the experimental uncertainty of the  $i$ th measurement point.

**2.1.1.2. Genetic algorithm.** Genetic algorithms are inspired by Darwin's theory of evolution and are used in this study to solve the optimization problem. The main outline of the algorithm, adapted for excavation problems by Levasseur [29] and summarized below, is based on the studies of Goldberg [20] and Renders [40].

Each soil parameter that will be optimized is binary encoded and represents a gene. In this study, the reference value for the primary deviatoric reference modulus,  $E_{50}^{ref}$  (defined by Brinkgreve [4]), represents a gene. The concatenation of several genes forms an individual. For instance, if  $E_{50}^{ref}$  of two soil layers are identified by the genetic algorithm, then the concatenation of two encoded  $E_{50}^{ref}$  values is called an individual. Each individual defines a point of search space. A group of  $N_i$  individuals represents a population of the  $i$ th generation.

A scalar error function  $F_{err}(p)$  is defined for each set of  $N_p$  unknown parameters, noted as a vector  $p$ . The minimization problem is solved in the  $N_p$ -dimension space restricted to a maximum and minimum value for each component of vector  $p$ .

The main stages of the genetic algorithm are shown in Fig. 1. In case that the  $F_{err}$  for the wall deformations and surface settlements is large, an evolutionary process such as using successively selection, reproduction and mutation of soil model parameters of interest (in this study  $E_{50}^{ref}$ ) is begun to generate new sets of soil model parameters [30]. These new sets are used in a forward analysis to compute deformations. This process is repeated until conditions of convergence (stop criteria) are satisfied: either the average of the error function on the parent part of the population is less than a given error or its standard deviation becomes small enough. More details of the analysis can be found in Levasseur [29] and Levasseur et al. [30–32].

**2.1.1.3. Principal component analysis.** After optimum soil model parameters based on the minimal value of the scalar error function are identified by GA, a principal component analysis [32] is conducted to evaluate the solution sets. This method is used to provide a representation of the solution sets identified by GA to make the comparison between several optimizations easier. The principal component analysis is a factorial analysis method which defines the main orientation of a set of the uncertain soil parameters, which in this study are the  $E_{50}^{ref}$  values within the research space. This orientation can be used to interpret the parameter sensitivities or to find correlations between parameters. By using PCA statistical analysis, from a discrete set of solution sets identified by GA, a continuous space of solution sets is estimated. An ellipsoid bounding sought after solution set is deduced from the principal component analysis. The area included in the ellipsoid is a first order mean linear approximation of the set of solutions identified by the GA optimization [32].

### 2.2. SelfSim learning inverse analysis

The autoprogressive algorithm was introduced by Ghaboussi et al. [16] to extract material constitutive behavior using complementary boundary measurements such as force and displacement. The SelfSim inverse analysis framework implements and extends the autoprogressive algorithm for the solution of a wide range of engineering problems. This inverse analysis approach has been used to extract material behavior from non-uniform material tests

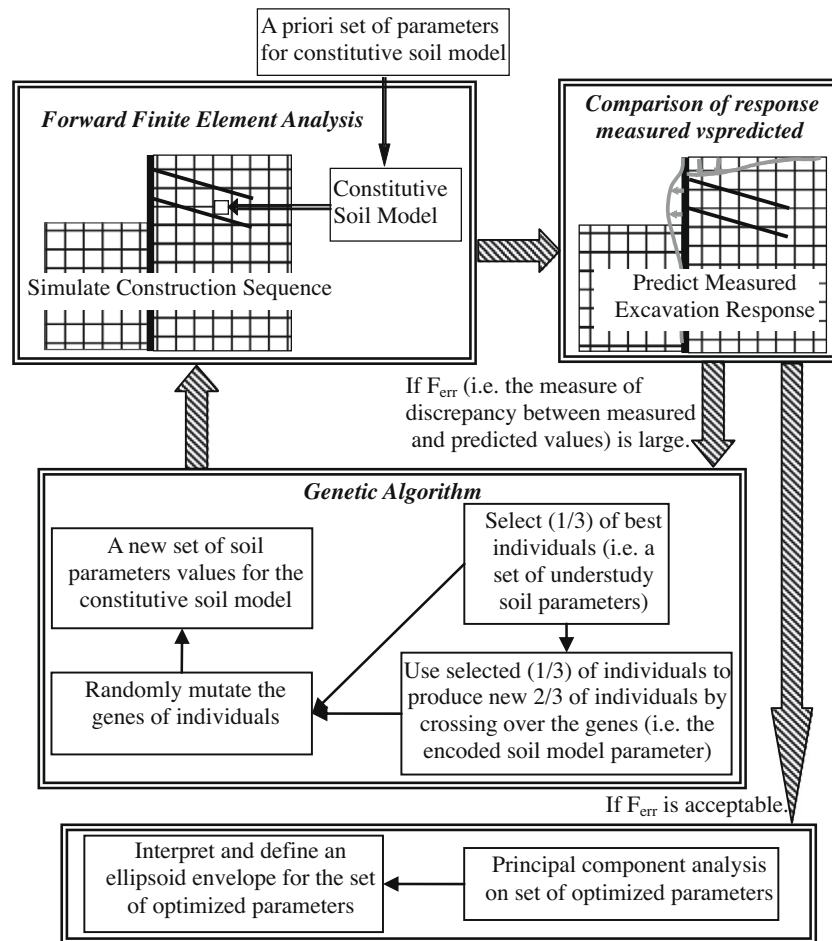


Fig. 1. Application of GA optimization to deep excavation problems.

[16,37,42,43] including laboratory triaxial tests with frictional ends [11,12,21] and is referred to as a self-learning concept [42]. Hashash et al. [22,23] demonstrated the feasibility of extracting material constitutive behavior from measurements of lateral wall deflections and surface settlements due to construction of a braced excavation.

The SelfSim framework as applied to excavation problems is illustrated in Fig. 2. Wall deformations and surface settlements are typically measured during excavations stages (Step 1). The measured deformations and the corresponding known excavation stage represent complementary sets of field observations. A numerical model is developed to simulate this pair of field observations. ABAQUS [1] is used as finite element engine for this method. The soil response is represented using a neural network (NN) based material constitutive model.

Prior to SelfSim learning the NN soil model is pretrained over a limited strain range using stress–strain data that represents linear elastic behavior. Laboratory tests or case histories also can be used for the pretraining.

In Step 2a of SelfSim, a finite element (FE) analysis is conducted to simulate soil removal and support installation for a given excavation stage using the current NN soil model. The stresses, strains and ground deformations such as wall deflections and surface settlements are computed. Most likely, the computed deformations will not match measured deformations. The computed strains are a poor approximation of the actual strains due to the discrepancy between computed and measured deformations. However due to equilibrium consideration and the use of correct force boundary conditions the corresponding stress field should provide an acceptable approximation of the actual stress field experienced by the soil.

In Step 2b of SelfSim a parallel FE analysis using the same NN soil model is performed whereby displacement boundary conditions such as wall deflection and surface settlements are imposed. The soil is also removed to reflect the current excavation stage. The computed stress field is expected to be a poor approximation of the actual stress field due to the discrepancy between computed and actual boundary forces. However, due to compatibility constraints and the use of accurate boundary displacements, the computed equilibrium strain field is an acceptable approximation of the actual strain field experienced by the soil.

The extracted stress field from Steps 2a and the extracted strain field from Step 2b form stress–strain pairs representing soil constitutive model and are used to retrain the NN soil model. The analyses of Step 2 and the subsequent NN model training are referred to as a SelfSim learning cycle.

For a given construction stage, several SelfSim learning cycles are conducted to extract a new set of stress–strain data for retraining of the current NN soil model. The solution converges when the analysis of Step 2a and 2b provide similar results. SelfSim cycles are conducted sequentially for all available construction stages and this is considered as a single SelfSim learning pass. Several SelfSim learning passes are conducted until the computed displacements match the measured values.

The SelfSim analyses presented by Hashash et al. [23] use lateral wall deflections and surface settlement measurements to capture excavation response and extract soil behavior. However, the SelfSim framework is not limited to these two types of measurements and can benefit from other measurements. Marulanda [33] concluded that additional instruments can potentially be used to develop a

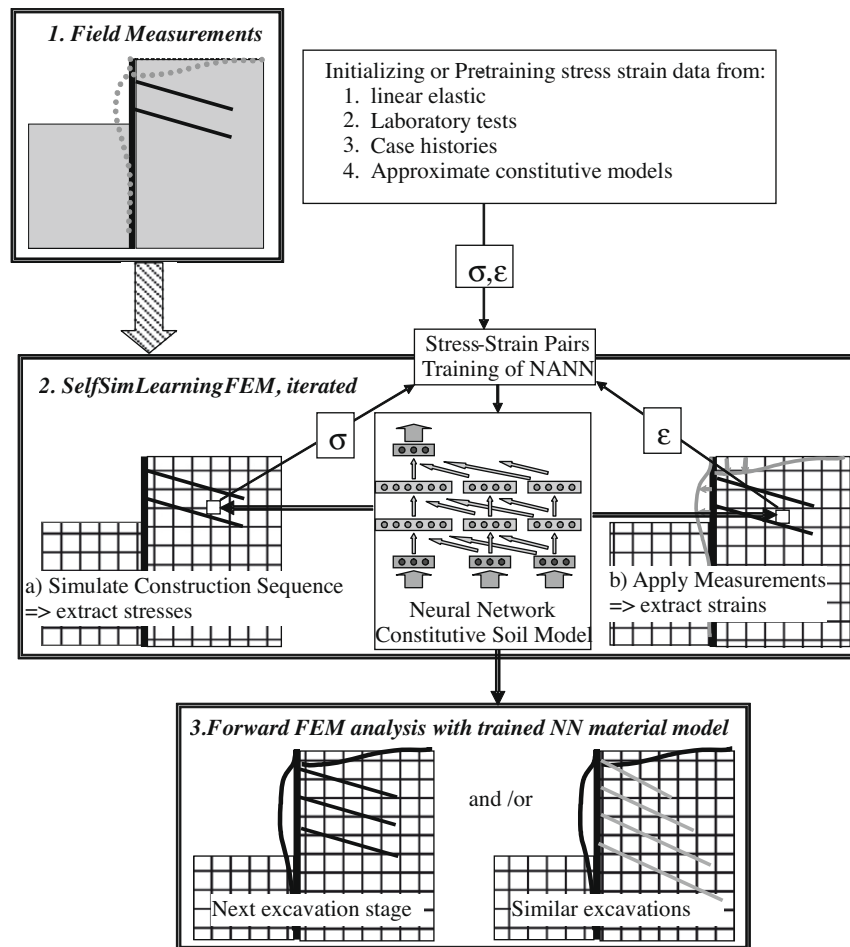


Fig. 2. Application of self-learning simulations to deep excavation problems.

more reliable extracted soil behavior. Song et al. [44] demonstrated that besides wall deformations, inclinometers placed at further distances back of the wall and strut loads are useful measurements that can improve learning soil behavior. The SelfSim framework can be conducted to extract the material behavior for both clayey and sandy soil sites. While the SelfSim framework has been applied to several clayey excavation sites [23], Osouli and Hashash [35] conducted SelfSim to extract sandy soil behavior from excavation measurements of a full scale model wall at Texas A&M supported by a two-level tieback section. The SelfSim approach has also been used to predict excavation-induced ground movements in several case studies [34]. Predicting excavation performances using developed model from SelfSim learning could be successful if the stress–strain ranges in predicted excavation fall in the learned stress–strain ranges. It is also noteworthy to mention that accuracy of the SelfSim analysis depends heavily on providing corresponding construction sequence to a measured field behavior.

### 3. Lurie Center excavation case study

#### 3.1. Geometry and instrument locations

The excavation for the Lurie Research Center was approximately 82 m by 69 m and depth of 13 m [10]. The site was heavily instrumented to monitor the ground movements resulting from the excavation. A plan view with instrument locations is shown in Fig. 3. The support system, typical soil profile at the site and element locations for stress paths plots are shown in Fig. 4. The element locations were

chosen close to inclinometer locations to have a better understanding of the soil displacement and the soil behavior simultaneously. The support system consisted of a sheet pile wall with three levels of tiebacks. The soil profile from the top consists of fill layer, lake sand layer, and soft to stiff silty clay layers.

Results from inclinometer LR1 were not used in the analyses due to proximity of the Prentice Pavilion building to this instrument location. Results from inclinometers LR3 and LR4 were not used in the analyses because of the presence of an existing, pile supported pedestrian tunnel in northwest corner of the site. Inclinometer LR2 was damaged during the construction. Corner effects influenced the results of inclinometer LR5, and hence were not amenable to plane strain simulations. Therefore inclinometer measurements obtained from LR6 and LR8 were considered amenable to a plane strain finite element simulation and were employed in GA and SelfSim inverse analyses.

Settlement data also were used for both inverse analyses. The settlement data correspond to average vertical displacements measured around the excavation. The excavation sequence was idealized into seven stages as shown in Fig. 5. The response of clayey layers was assumed to be undrained during excavation. The excavation was simulated down to El. –7.3 m.

#### 3.2. Learning of global excavation response using optimization approach based on GA

In the optimization approach based on GA, each soil layer is modeled by the constitutive hardening soil model of PLAXIS [4].

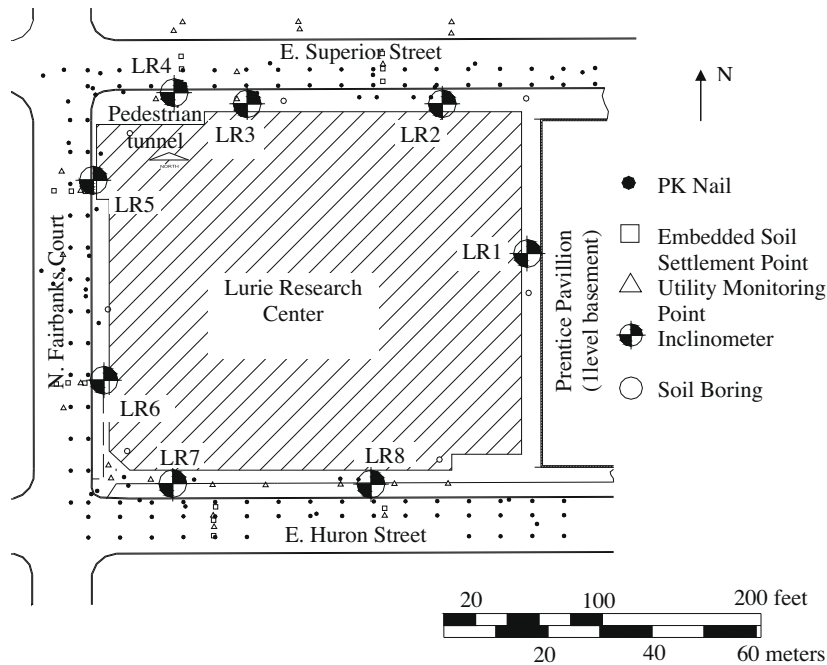


Fig. 3. Plan view and instrument locations of Lurie Center excavation.

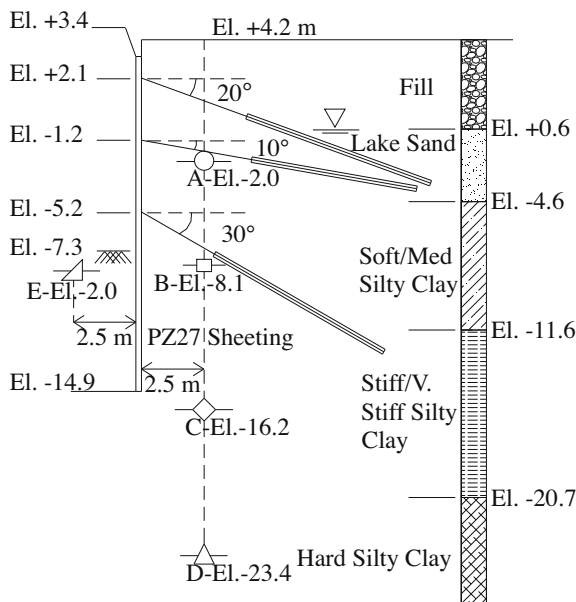


Fig. 4. Cross section of the wall, soil layers and location of elements for extracted stress paths.

For volumetric hardening, an elliptical yield function is used and an associated flow rule is assumed. For shear hardening, a yield function of hyperbolic type and a non-associated flow rule that incorporates a dilation angle is employed. The field observations used in the optimization analysis are selected from inclinometers measurements and surface settlements at stage 7 of the excavation.

Since the stiffness of stiff clay is different around the excavation [5] and the primary deviatoric modulus ( $E_{50}^{ref}$ ), in the soft to medium clay layer and in the stiff clay layer, are the most influential parameters on the behavior of the excavation [9], ( $E_{50}^{ref}$ ) of soft to medium clay layer and the stiff clay layer are identified by GA approach. The other soil parameters do not play a significant role in controlling sheet pile wall behavior, and thus the corresponding

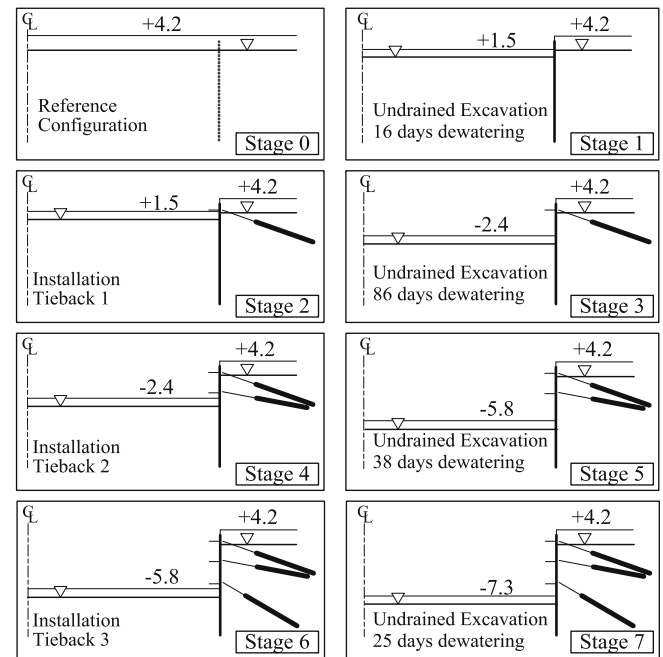


Fig. 5. Construction sequence of Lurie Center excavation site.

hardening soil parameters can be fixed according to literature on Chicago clays [7]. The ( $E_{50}^{ref}$ ) of fill layer is also identified, because surface settlements are used in the inverse analysis. The other hardening soil model parameters for Chicago clays are kept fixed, and are shown in Table 1.

The range of ( $E_{50}^{ref}$ )<sub>fill</sub>, ( $E_{50}^{ref}$ )<sub>med</sub>, and ( $E_{50}^{ref}$ )<sub>stiff</sub> values in each layer is assumed to be:

$$3000 \leq (E_{50}^{ref})_{fill} \leq 35,000 \text{ kPa}$$

$$3000 \leq (E_{50}^{ref})_{medium \text{ clay}} \leq 35,000 \text{ kPa}$$

$$40,000 \leq (E_{50}^{ref})_{stiff \text{ clay}} \leq 200,000 \text{ kPa}$$



**Table 1**

Hardening soil parameters for each soil layers of the Lurie Center.

Hardening soil parameters	Fill layer	Lake sand layer	Soft to medium clay layer	Stiff clay layer	Hard clay layer
Type	Drained	Drained	Undrained	Undrained	Undrained
$E_{50}^{\text{ref}}$ (kPa)	Studied parameter	48,000	Studied parameter	Studied parameter	$(1.5 \cdot E_{50}^{\text{ref}})_{\text{stiff}}$
$E_{\text{oed}}^{\text{ref}}$ (kPa)	13,500 <sup>a</sup>	48,000 <sup>a</sup>	$0.7 \cdot E_{50}^{\text{ref}}$ <sup>a</sup>	$0.7 \cdot E_{50}^{\text{ref}}$ <sup>a</sup>	$0.7 \cdot E_{50}^{\text{ref}}$ <sup>a</sup>
$E_{\text{ur}}^{\text{ref}}$ (kPa)	40,500 <sup>a</sup>	144,000 <sup>a</sup>	$3.5 \cdot E_{50}^{\text{ref}}$ <sup>a</sup>	$3 \cdot E_{50}^{\text{ref}}$ <sup>a</sup>	$3 \cdot E_{50}^{\text{ref}}$ <sup>a</sup>
Power coefficient $m$	0.5	0.5	0.8 <sup>a</sup>	0.85 <sup>a</sup>	0.6
$p^{\text{ref}}$ (kPa)	100 <sup>a</sup>	100 <sup>a</sup>	100 <sup>a</sup>	100 <sup>a</sup>	100 <sup>a</sup>
Cohesion, $c$ (kPa)	19	0.2 <sup>a</sup>	0.2 <sup>a</sup>	0.2 <sup>a</sup>	0.2 <sup>a</sup>
Friction angle, $\phi$ (°) <sup>d</sup>	30	35 <sup>c</sup>	26 <sup>a</sup>	32 <sup>a</sup>	35 <sup>c</sup>
Dilat. angle, $\psi$ (°)	2	5 <sup>a</sup>	0 <sup>a</sup>	0 <sup>a</sup>	0 <sup>a</sup>
$v_{\text{ur}}$	0.2 <sup>a</sup>	0.2 <sup>a</sup>	0.2 <sup>a</sup>	0.2 <sup>a</sup>	0.2 <sup>a</sup>
OCR	1 <sup>b</sup>	1.1 <sup>b</sup>	1.4 <sup>b</sup>	1.5 <sup>b</sup>	2.5 <sup>b</sup>

<sup>a</sup> Ref. [6].<sup>b</sup> Ref. [7].<sup>c</sup> Ref. [9].<sup>d</sup> The converted friction angles of lake sand, soft to medium clay, stiff clay and hard clay for plain strain condition are considered 40°, 30°, 36°, and 39° respectively. [28,38,46].

These intervals define the boundaries of the research space for GA optimization. The increment changes of the parameters in this research spaces are as follows:  $\Delta(E_{50}^{\text{ref}})_{\text{med}} = \Delta(E_{50}^{\text{ref}})_{\text{fill}} = 500$  kPa and  $\Delta(E_{50}^{\text{ref}})_{\text{stiff}} = 2500$  kPa. According to this research space and measured deformations of the excavation, a solution set is identified by GA as shown in Fig. 6. The convergence for this analysis takes about 2 days with an office computer. From this set, an ellipsoid is estimated by PCA, Fig. 6. The ellipsoids characterize the solution set. Fig. 6 shows that two ellipsoids are elongated in the directions of  $(E_{50}^{\text{ref}})_{\text{stiff}}$  and  $(E_{50}^{\text{ref}})_{\text{fill}}$ , which implies the model is more sensitive to the medium clay modulus,  $(E_{50}^{\text{ref}})_{\text{med}}$ , than to moduli of fill and stiff clay layer. Notice that this result confirms that stiff clay modulus,  $(E_{50}^{\text{ref}})_{\text{stiff}}$ , varied around the excavation. Therefore, its identification by inverse analysis is very difficult. In this set, the optimal parameter values estimated by GA are as followings:

$$(E_{50}^{\text{ref}})_{\text{fill}} = 28,000 \text{ kPa}$$

$$(E_{50}^{\text{ref}})_{\text{medium clay}} = 5500 \text{ kPa}$$

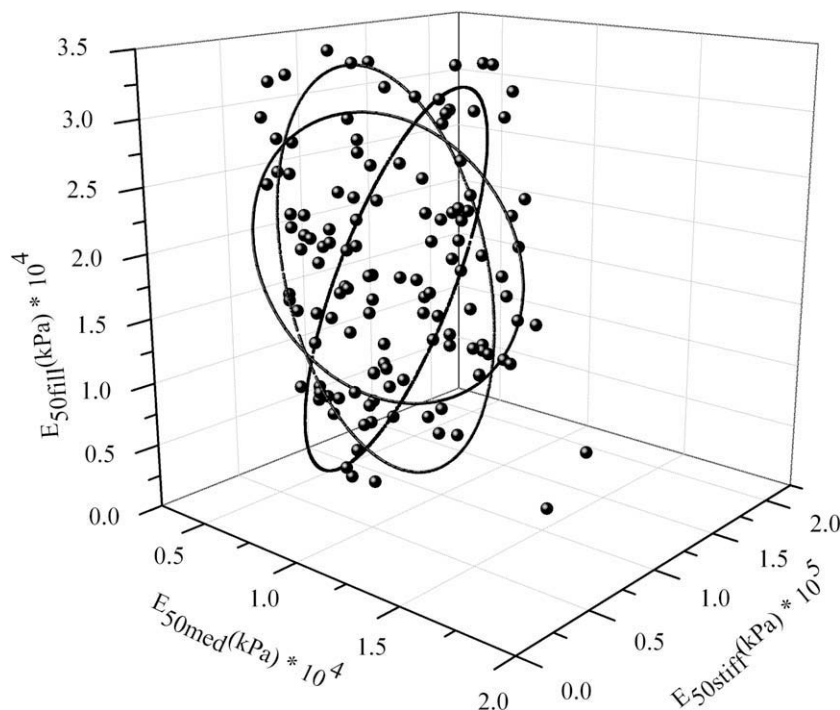
$$(E_{50}^{\text{ref}})_{\text{stiff clay}} = 172,500 \text{ kPa}$$

Fig. 7 shows that these parameter values reproduce the horizontal displacements measured by the inclinometers as well as the observed settlements for stage 7 of the excavation reasonably well.

### 3.3. Learning of global excavation response using SelfSim learning approach

SelfSim is applied to the Lurie Research Center whereby lateral soil movements in proximity to the wall and surface settlements corresponding to the known construction stages for all stages of the excavation are used as boundary conditions for SelfSim learning. The inclinometers were located 5 ft behind the sheetpile wall, and therefore the lateral deflections used during SelfSim learning are applied in the finite element analysis at the same location for all elevations. Each soil layer is modeled with a different NN soil model.

Prior to any learning, an initial soil constitutive model using the NN base module is developed to represent linear elastic response

**Fig. 6.** Solution set identified by GA and estimated ellipsoid using wall deformation and surface settlements.

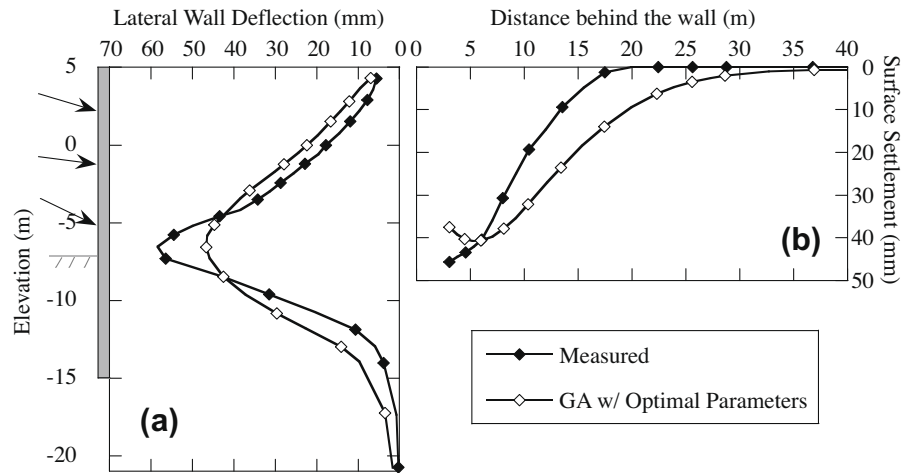


Fig. 7. Comparison of computed (a) lateral wall deformation and (b) surface settlement using GA method with optimal parameter values.

within a strain range of 0.1%. This analysis underestimates lateral wall deformations and surface settlements, but gives a qualitatively reasonable deformed shape. Several SelfSim learning cycles are conducted at each excavation stage. After a few passes of SelfSim learning, the calculated deformations match reasonably with the measured values. In SelfSim analysis there are no soil parameters to optimize, and the soil behavior is captured through data bases of stress–strain pairs.

Fig. 8 shows the deformations after 12 SelfSim learning passes [23]. This SelfSim learning takes about few hours with an office computer. The computed deformations using soil models extracted through SelfSim learning are similar to the field measurements, although there are some noticeable discrepancies in the initial two stages between the computed and the measured soil movements. One possible reason for these differences is the large measured surface settlement associated with the behavior of the pavement material and/or near-surface fill. These relatively large surface settlements at the early stages were likely caused by cyclic motions induced by the vibratory hammer used to install the sheeting, and thus are not considered in the learning process.

### 3.4. Comparison of global excavation response

Comparison of computed lateral deformations and surface settlement from GA and SelfSim for the stage 7 of excavation are shown in Fig. 9. Since both analyses used the inclinometer measurement of the stage 7 of excavation, computed lateral deformation of SelfSim and genetic algorithm match reasonably with the measurements.

Although the settlement profile was also used in GA optimization analysis, it appears that the hardening soil model used in the FE model is not capable of reproducing the settlement profile behind the wall, neither in magnitude nor in shape. The hardening soil model version used in this study does not have small strain non-linearity and thus could not represent the stiffness variation over the range of strain levels that diminishes with further distance from the wall. Therefore, the computed surface settlements do not perfectly match with the measured values. Notice that in this case, GA optimization based only on horizontal displacements provides the same optimal parameters compared to the optimization based on horizontal displacements and settlements.

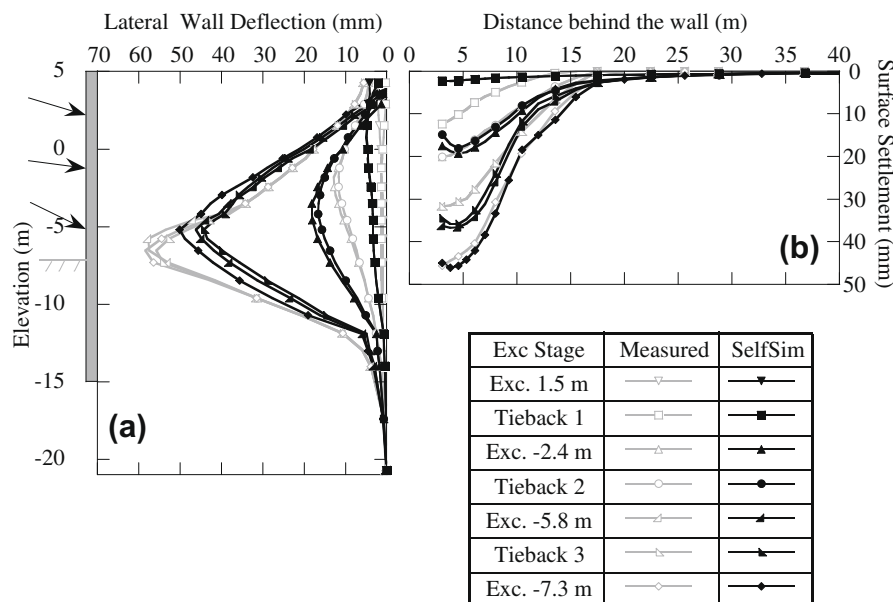


Fig. 8. Computed (a) lateral wall deformations and (b) surface settlements after 12 passes of SelfSim learning.

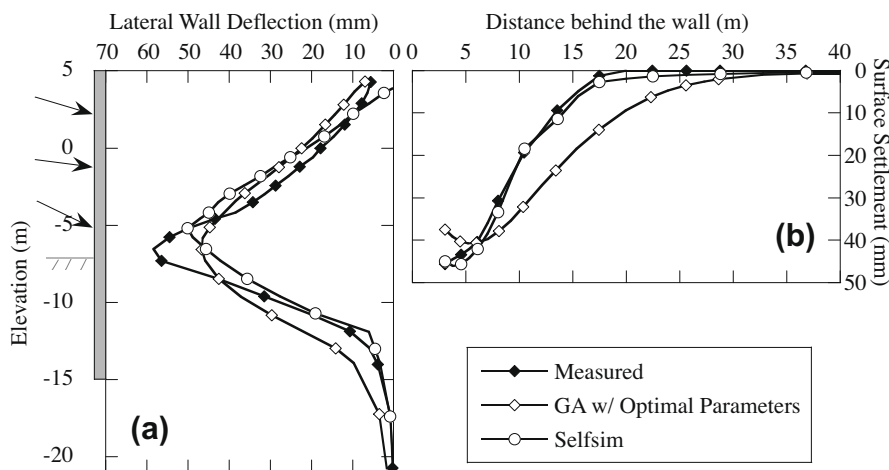


Fig. 9. Comparison of computed (a) lateral wall deformation and (b) surface settlement using GA and SelfSim for the stage 7 of excavation.

Since SelfSim is not pre constrained to the limitation of a conventional constitutive model, it can capture the settlements more reasonably. SelfSim can also provide computed deformations in intermediate stages of excavation.

### 3.5. Comparison of extracted soil behavior after GA and SelfSim learning

The stress paths for selected elements, shown in Fig. 4, are compared in Fig. 10. It is observed that stress paths in the clay layers primarily are elastic. This confirms Finno and Calvello [9] conclusions that the primary deviatoric loadings  $E_{ref}^{50}$  have the most influence on the behavior of an excavation through the compressible clays in Chicago.

The stress paths before and after SelfSim learning are illustrated in Fig. 11. The NN soil model evolved from reflecting linear elastic soil response, such that it is able to learn relevant soil behavior, including small strain non-linearity, essential to compute the shape of the settlement trough. The stress paths for the top soft

layers are more non-linear than the bottom layers. The comparison of Figs. 10 and 11 show that in unloading condition (i.e. element E), the extracted soil behavior from both analyses is closer to an elastic response. For elements located in retained soil (i.e. elements A, B, C, D), the mean stress extracted from SelfSim analysis is decreasing with shearing during the excavation steps. The SelfSim extracted stress paths demonstrate a non-linear response for all clay layers and the sand layer. The SelfSim analysis shows that elements A, B and C undergo shearing almost identical to the plane strain active (PSA) mode. Elements A and B in the retained soil reach the peak strength and then experience unloading [25]. However the mean stress from GA analysis is constant for all clayey layers except than the sand layer during the excavation. Therefore the stress paths from GA analysis for all clay layers show qualitatively an elastic behavior.

Fig. 12 shows the comparison of stress paths after using genetic algorithm and SelfSim learning for the lake sand layer. The friction angle envelope is shown in this figure. Under plane strain conditions, the out-of-plane component of strain is equal to zero. This

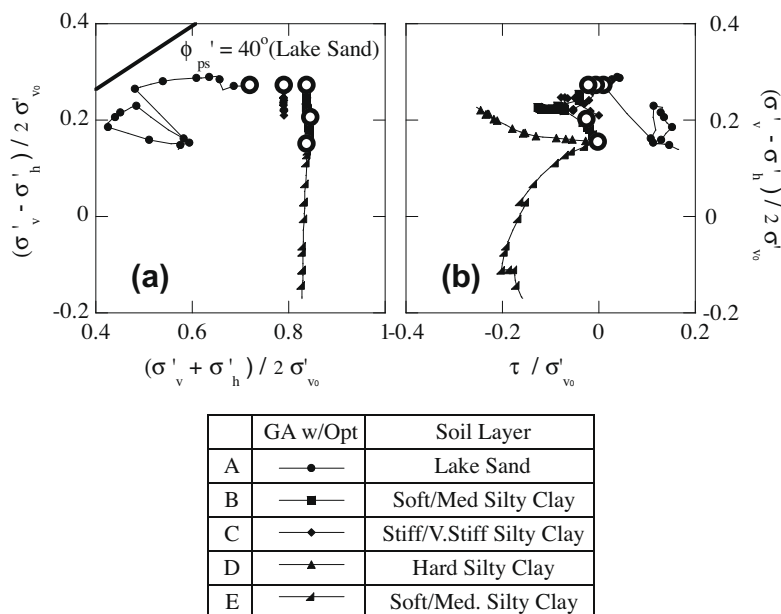


Fig. 10. Normalized stress paths of (a)  $p'$ – $q$ , and (b)  $\tau$ – $q$  for elements A, B, C, D, and E after using GA analysis method with optimal parameter values and average parameter values.



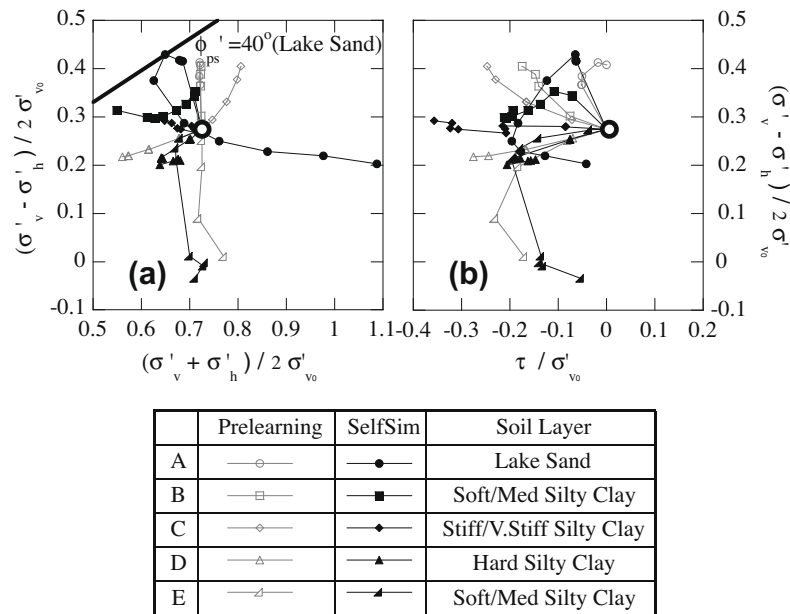


Fig. 11. Normalized stress paths of (a)  $p'$ - $q$ , and (b)  $\tau$ - $q$  for elements A, B, C, D, and E before and after SelfSim learning.

constraint reduces the degree of freedom that individual soil particles can move in relation to one another, thus increasing geometric influence [46]. Therefore the triaxial friction angle is converted to plane strain friction angles as indicated in Table 1. Both analyses show a non-linear stress path for the lake sand layer. SelfSim analysis does not use any pre-defined stress strain relationship, nevertheless the stress paths for SelfSim analysis show that stress paths do not exceed the failure envelope.

Fig. 13 shows the comparison of stress paths using genetic algorithm and SelfSim learning for clay layers. For simplicity in SelfSim learning the coefficient of earth pressure at-rest is constant through the soil layers, but in genetic algorithm the coefficient of earth pressure is varied through the soil layers. Genetic algorithm analysis shows an elastic stress path for all clay layers. The stress paths obtained after SelfSim learning for clay layers show a distinct non-linear soil behavior. This observation can explain why the surface settlement predictions in genetic algorithm are not as accurate as settlement predictions in SelfSim. Since the small strain non-linearity of soil is reasonably captured with SelfSim learning approach, the surface settlement match with the measured values

[23,44]. The stress path for all clay layers particularly element B which is in soft/med clay layer shows that stresses paths do not exceed failure envelope.

Both GA and SelfSim could reproduce the wall deformations reasonably well; however comparison of stress paths show that SelfSim approach could extract the underlying soil behavior more reasonably than hardening soil model used in the GA optimization approach. The outcome would differ if a different material constitutive model is used in the GA approach.

SelfSim learning is based on soil horizontal displacement measurements and settlements which permit the capture of the soil non-linear behavior. However, this method is independent of any constitutive model. On contrary, GA optimization is based on the calibration of an existing soil constitutive model on soil horizontal displacement measurements and settlements. This method permits the use of well known conventional geotechnical models (often used in engineering) from which some of parameters can be evaluated independently to the optimization. However, the choice of the constitutive model mainly influences the final soil behavior in GA optimization. This choice is the main limitation of the method as

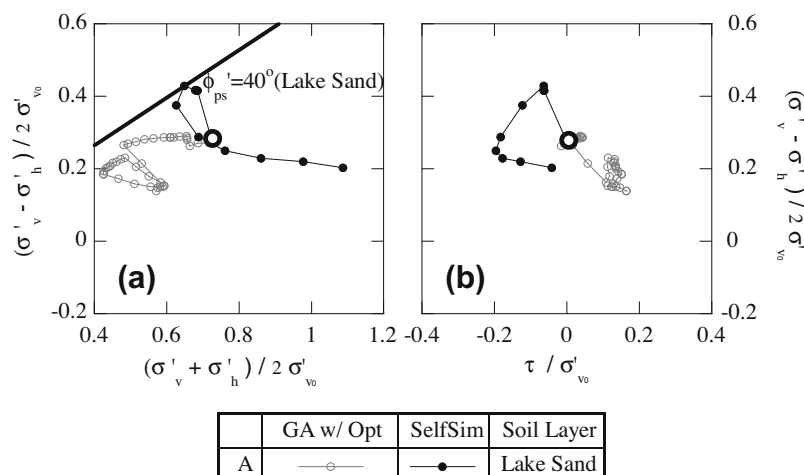


Fig. 12. Normalized stress paths comparison of (a)  $p'$ - $q$ , and (b)  $\tau$ - $q$  for element A after using GA with optimal parameter values and SelfSim in lake sand layer.

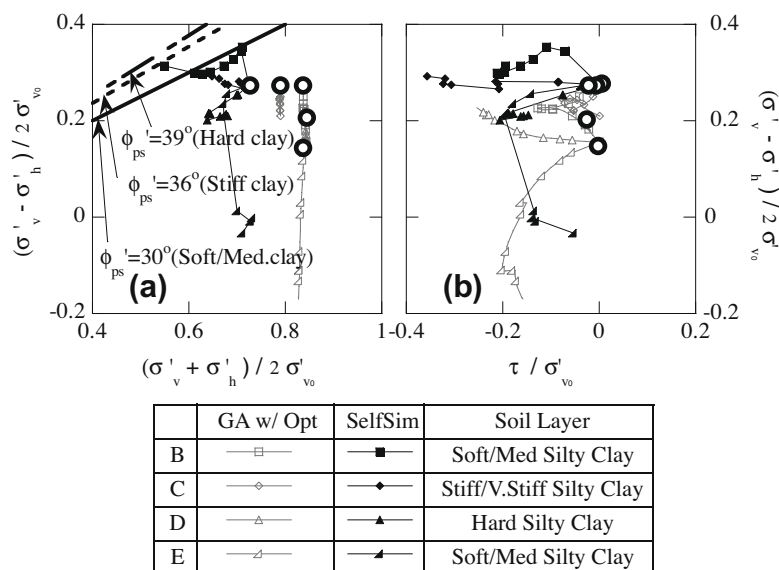


Fig. 13. Normalized stress paths comparison of (a)  $p'$ - $q$ , and (b)  $\tau$ - $q$  for elements B, C, D, and E after using GA with optimal parameter values and SelfSim in clay layers.

shown in Levasseur et al. [31,32]. If more advanced models that have relevant aspects of soil behavior such as small strain non-linearity are used, the GA optimization is expected to capture excavation response including small strain non-linearity more accurately. SelfSim allows for the discovery of new material behavior while GA optimization assists engineers in use of existing material models through a better selection of material model parameters.

#### 4. Conclusions

Field data are integrated with numerical models to simulate complex geotechnical problems. Inverse analysis techniques are powerful numerical tools to evaluate performance of geotechnical structures and extract soil behaviors. Two inverse analysis methods are evaluated using measured data collected at the Lurie Center case study in Chicago. Optimized parameters found from the GA approach and the learned constitutive responses from SelfSim formed the basis of simulations that could reasonably compute deformations observed during the excavation for the Lurie Center. Unlike GA analysis in which the soil model has to be pre-constrained to specific model (in this study soil hardening model), SelfSim analysis is able to produce continuously evolving material models that can learn new material behavior. This capability allows SelfSim to capture the underlying soil behavior learning measurements at different construction stages. Optimization based on genetic algorithm could predict the inclinometer measurements very well, but the stress paths for this method show linear elastic behavior for clay layers, a feature of the hardening soil model and the undrained simulation. On the other hand SelfSim is able to capture nonlinearity of soil behavior. This feature explains why the NN material model is able to compute settlement profile reasonably well. The computational demands of both methods vary, though they require skilled users. SelfSim allows for the discovery of new material behavior while GA optimization assists engineers in use of existing material models through a better selection of material model parameters.

#### Acknowledgements

This material is based upon work supported by the National Science Foundation under Grant No. CMS 02-19123 under program director Dr. R. Frigaszy. Any opinions, findings, and conclusions

or recommendations expressed in this material are those of the writers and do not necessarily reflect the views of the National Science Foundation.

#### Reference

- ABAQUS. ABAQUS/Standard, A general purpose finite element code. Pawtucket (RI): ABAQUS, Inc., formerly Hibbitt, Karlsson & Sorensen, Inc.; 2005.
- Anandarajah A, Agarwal D. Computer-aided calibration of a soil plasticity model. *Int J Numer Anal Methods Geomech* 1991;15(12):835–56.
- Arai K, Ohta H, Kojima K. Application of back analysis to several test embankments on soft clay deposits. *Soil Found* 1986;26(2):60–72.
- Brinkgreve RBJ. Plaxis v8; 2003.
- Calvello M. Inverse analysis of a supported excavation through Chicago glacial clays. Evanston (IL): Northwestern University; 2002.
- Calvello M, Finno RJ. Selecting parameters to optimize in model calibration by inverse analysis. *Comput Geotech* 2004;31(5):410–24.
- Chung CK, Finno RJ. Influence of depositional processes on the geotechnical parameters of Chicago glacial clay. *Eng Geol* 1992;32:225–42.
- Cividini A, Rossi AZ. The consolidation problem treated by a consistent (static) finite element approach. *Int J Numer Anal Methods Geomech* 1983;7:435–55.
- Finno RJ, Calvello M. Supported excavations: observational method and inverse modeling. *J Geotech Geoenviron Eng* 2005;131(7):826–36.
- Finno RJ, Roboski JF. Three-dimensional responses of a tiedback excavation through clay. *J Geotech Geoenviron Eng* 2005;131(3):272–83.
- Fu Q, Hashash YMA, Ghaboussi J. Non-uniformity of stress states within a dense sand specimen. In: *Geo-Denver 2007*, Denver, Co.; 2007.
- Fu Q, Hashash YMA, Jung S, Ghaboussi J. Integration of laboratory testing and constitutive modeling of soils. *Comput Geotech* 2007;34(5):330–45.
- Gens A, Ledesma A, Alonso EE. Estimation of parameters in geotechnical back analysis. 2. Application to a tunnel excavation problem. *Comput Geotech* 1996;18(1):29–46.
- Ghaboussi J. Biologically inspired soft computing methods in structural mechanics and engineering. *Struct Eng Mech* 2001;11(5):485–502.
- Ghaboussi J, Garrett JH, Wu X. Knowledge-based modeling of material behaviour with neural networks. *J Eng Mech Div* 1991;117(1):132–53.
- Ghaboussi J, Pecknold DA, Zhang MF, Haj-Ali RM. Autoprogessive training of neural network constitutive models. *Int J Numer Methods Eng* 1998;42(1):105–26.
- Ghaboussi J, Sidarta DE. New method of material modeling using neural networks. In: *Sixth international symposium on numerical models in geomechanics*, Montreal, Canada; 1997.
- Gioda G, Locatelli L. Back analysis of the measurements performed during the excavation of a shallow tunnel in sand. *Int J Numer Anal Methods Geomech* 1999;23:1407–25.
- Gioda G, Sakurai S. Back analysis procedures for the interpretation of field measurements in geomechanics. *Int J Numer Anal Methods Geomech* 1987;11:555–83.
- Goldberg DE. Genetic algorithms in search, optimization and machine learning. Addison Wesley Publishing Company; 1989.
- Hashash YMA, Fu Q, Ghaboussi J, Lade PV, Saucier C. Inverse analysis based interpretation of sand behavior from triaxial shear tests subjected to full end restraint. *Canadian Geotech J*, in press.

- [22] Hashash YMA, Marulanda C, Ghaboussi J, Jung S. Systematic update of a deep excavation model using field performance data. *Comput Geotech* 2003;30:477–88.
- [23] Hashash YMA, Marulanda C, Ghaboussi J, Jung S. Novel approach to integration of numerical modeling and field observations for deep excavations. *J Geotech Geoenviron Eng* 2006;132(8):1019–31.
- [24] Hashash YMA, Whittle AJ. Ground movement prediction for deep excavations in soft clay. *J Geotech Eng* 1996;122(6):474–86.
- [25] Hashash YMA, Whittle AJ. Mechanisms of load transfer and arching for braced excavations in clay. *J Geotech Geoenviron Eng* 2002;128(3):187–97.
- [26] Honjo Y, Wen-Tsung L, Guha S. Inverse analysis of an embankment on soft clay by extended Bayesian method. *Int J Numer Anal Methods Geomech* 1994;18:709–34.
- [27] Jolliffe IT. *Principal component analysis*. NY; 2002.
- [28] Ladd CC, Edgers L. Consolidated-undrained direct simple shear test on Boston Blue Clay. Research report R72-82. Department of Civil Engineering, MIT, Cambridge, MA; 1972.
- [29] Levasseur S. *Analyse inverse en geotechnique: developement d'une methode base d'algorithmes genetiques*. Grenoble, France: Universite Joseph Fourier, 2007.
- [30] Levasseur S, Malecot Y, Boulon M, Flavigny E. Soil parameter identification using a genetic algorithm. *Int J Numer Anal Methods Geomech* 2008;32(2):189–213.
- [31] Levasseur S, Malecot Y, Boulon M, Flavigny E. Statistical inverse analysis based on genetic algorithm and principal component analysis: method and developments using synthetic data. *Int J Numer Anal Methods Geomech* 2009;33(12):1485–511.
- [32] Levasseur S, Malecot Y, Boulon M, Flavigny E. Statistical inverse analysis based on genetic algorithm and principal component analysis: applications to excavation problems and pressuremeter tests. *Int J Numer Anal Methods Geomech*, in press. doi: 10.1002/nag.776.
- [33] Marulanda C. Integration of numerical modeling and field observations of deep excavations. Civil and Environmental Engineering, Urbana, University of Illinois at Urbana-Champaign; 2005. 269 p.
- [34] Osouli A. The interplay between field measurements and soil behavior for learning supported excavation response. Civil and Environmental Engineering, Ph.D. Thesis, Urbana, University of Illinois at Urbana-Champaign; 2009.
- [35] Osouli A, Hashash YMA. Learning of soil behavior from measured response of a full scale test wall in sandy soil. In: 6th International conference on case histories in geotechnical engineering, Arlington, VA, August 11–16, 2008.
- [36] Ou CY, Tang YG. Soil parameter determination for deep excavation analysis by optimization. *J Chinese Inst Eng* 1994;17(5):671–88.
- [37] Pande GN, Shin HS. Finite elements with artificial intelligence. In: Eighth international symposium on numerical models in geomechanics – NUMOG VIII. Italy: Balkema; 2002.
- [38] Pestana JM, Whittle AJ, Gens A. Evaluation of a constitutive model for clays and sands: part II – clay behaviour. *Int J Numer Anal Methods Geomech* 2002;26(11):1123–46.
- [39] PLAXIS-B.V. *PLAXIS: finite element package for analysis of geotechnical structures*. Delft, Netherland; 2002.
- [40] Renders JM. *Algorithmes genetiques et reseaux de neurones*. Hermes; 1994.
- [41] Samarajiva P, Macari EJ, Wathugala W. Genetic algorithms for the calibration of constitutive models of soils. *Int J Geomech* 2005;5(3):206–17.
- [42] Shin HS, Pande GN. On self-learning finite element codes based on monitored response of structures. *Comput Geotech* 2000;27(7):161–78.
- [43] Sidarta DE, Ghaboussi J. Constitutive modeling of geomaterials from non-uniform material tests. *Int J Comput Geotech* 1998;22(1):53–71.
- [44] Song H, Osouli A, Hashash Y. Soil behavior and excavation instrumentation layout. In: 7th International symposium on field measurements in geomechanics FMGM 2007, Boston, MA; 2007.
- [45] Tarantola A. *Inverse problem theory*. Elsevier Science BV; 1987.
- [46] Terzaghi K, Peck RB, Mesri G. *Soil mechanics in engineering practice*. New York: Wiley; 1996.
- [47] Zadeh LA. Fuzzy logic, neural networks, and soft computing. *Commun ACM* 1997;37(3):77–84.
- [48] Zentar R, Hicher PY, Moulin G. Identification of soil parameters by inverse analysis. *Comput Geotech* 2001;28:129–44.